The Vinylketene–Acylallene Rearrangement: Theory and Experiment

Hervé Bibas, Ming Wah Wong,* and Curt Wentrup*

Abstract: Alkoxyvinylketenes **4** are generated by flash vacuum thermolysis (FVT) or photolysis of 3-alkoxycyclobutenones **3**. The thermal interconversion of **4** and allene carboxylic acid esters **5** under FVT conditions is demonstrated by Ar matrix FTIR spectroscopy. In addition, ethoxyvinylketene **4b** undergoes thermal elimination of ethene with formation of *s-cis*- and *s-trans*-acetylketene (**8**). An analogous aminovinylketene-to-allenecarboxamide conversion is observed on FVT of 3-dimethylaminocyclobutenone **3c**. A facile 1,3-chlorine migration in 2,3-butadienoyl chloride (**5d**) is also reported. Consistent with the experimental observations, 1,3-methoxy, 1,3-chloro, and 1,3-dimethylamino migrations in vinylketene are calculated (G2(MP2,SVP) level) to have moderate barriers of 169, 157, and 129 kJ mol^{-1}, respectively, significantly less than the corresponding 1,3-H shift barrier (273 kJ mol^{-1}). The stabilization of the four-center transition structures is rationalized in terms of the donor–acceptor interaction between the lone pair electrons of the migrating donor substituent and the vacant central carbon p orbital of the ketene LUMO. The predicted migratory aptitude in the series of substituted vinylketenes, R-C(=CH_2)-CH=C=O, is in the order $N(CH_3)_2 > SCH_3 > SH > Cl > NH_2 > OCH_3 > OH > F > H > CH_3$, and correlates well with the electron-donating ability of the R group.

Keywords
ab initio calculations · allenes · ketenes · matrix isolation · rearrangements

Introduction

The chemistry of ketenes has been of much interest recently.[1] In previous work, we have shown that α-oxoketenes (acylketenes) (**1a**) undergo a degenerate thermal rearrangement involving a 1,3-shift of the group R (Scheme 1).[2, 3] This migration is

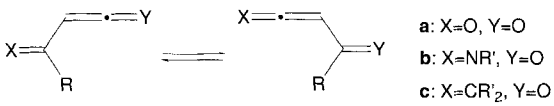

Scheme 1.

dramatically accelerated for electron-donating substituents R (OR′, SR′, and NR'_2) owing to a favorable overlap between the lone pair of the migrating atom and the vacant central carbon p orbital of the ketene LUMO.[3] A similar reaction interconverts imidoylketenes (**1b**) and α-oxoketenimines (**2b**).[4] Further computational work indicates that the activation barriers are related to the electrophilicities of the carbon atoms where the migration occurs.[5] Thus, for 1,3-H migration, the activation barrier increases along the series α-oxoketene < α-oxoketenimine < imidoylketene. It is intriguing to ask whether a similar 1,3-migration is possible for the vinyl analogues, which interconverts vinylketenes (**1c**) and acylallenes (**2c**).

In this paper, we provide experimental evidence for the 1,3-migrations of methoxy, ethoxy, dimethylamino, and chlorine substituents in vinylketene (**1c**).[6] Ab initio calculations of the reaction profiles for the vinylketene–acylallene rearrangements were carried out to elucidate the mechanism of the 1,3-migration and to predict the migratory aptitude for a series of substituted vinylketenes (R-C(=CH_2)-CH=C=O).

Results and Discussion

1. Alkoxy groups: 3-Methoxycyclobutenone[7] (**3a**) underwent flash vacuum thermolysis (FVT)[8] at temperatures above 400 °C to give the *s-cis*- and *s-trans*-methoxyvinylketenes[9] (**4a**, Scheme 2), as evidenced by Ar matrix isolation of the ketenes at 12 K. The characteristic bands are at 2134 and 2142 cm^{-1} for *s-cis*- and *s-trans*-**4a**, respectively. The band at 2138 cm^{-1} appears to be due to a site of *s-trans*-**4a** (Figure 1a). These assignments are discussed below. At 77 K (neat deposition), a single band at 2123 cm^{-1} is observed. A direct comparison of the full spectrum of **4a**, generated by FVT at 500 °C and deposited in Ar matrix at 12 K, with the calculated IR spectrum of *s-trans*-**4a** shows that the *s-trans* conformer is the main species formed (Figure 2; Table 1). It appears that the band at 2142 cm^{-1} is the main absorption of the *s-trans* vinylketene. Comparison of the intensities of the bands in the experimental spectrum with those

[*] Prof. C. Wentrup, Dr. M. W. Wong, H. Bibas
Department of Chemistry, The University of Queensland
Brisbane, QLD 4072 (Australia)
Fax: Int. code +(7)3365-4580
e-mail: wentrup@chem.chemistry.uq.edu.au

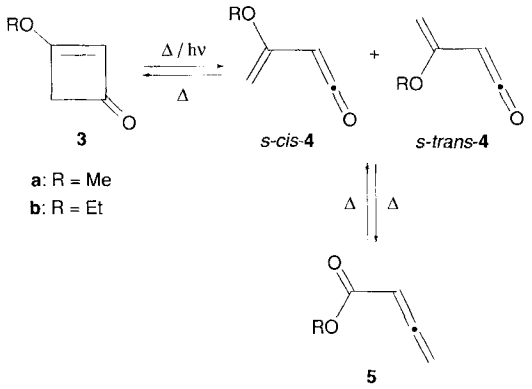

Scheme 2.

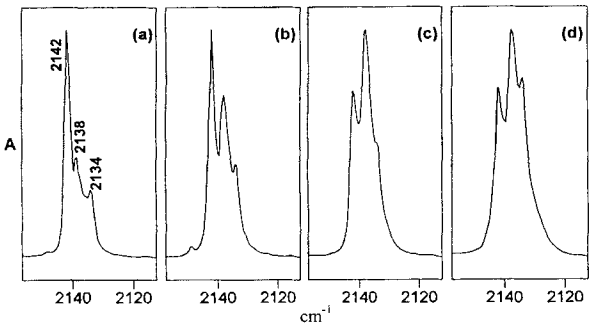

Figure 1. Partial Ar matrix FTIR spectra (12 K) of the results of FVT of **3a** under different conditions (T_o = oven T (°C), T_d = deposition T (°C), V = vacuum (mbar), t_d = deposition time (min), P = pressure of argon used during deposition (mbar)): a) $T_o = 500$, $T_d = -17$, $V = 2\times10^{-5}$, $t_d = 19$, $P = 190$; b) $T_o = 540$, $T_d = -18$, $V = 10^{-5}$, $t_d = 25$, $P = 155$; c) $T_o = 420$, $T_d = -15$, $V = 2\times10^{-5}$, $t_d = 15$, $P = 50$; d) $T_o = 450$, $T_d = -14$, $V = 3\times10^{-5}$, $t_d = 10$, $P = 100$ (deposition T: 17 K). Peak assignment: 2142, *s-trans*-**4a**; 2138, a site of *s-trans*-**4a**; 2134, *s-cis*-**4a** (appears to have a contribution from a second site of *s-trans*-**4a**.

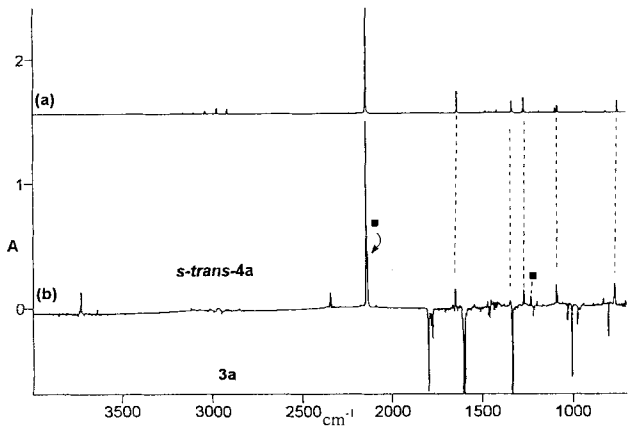

Figure 2. IR spectra of *s-trans*-**4a**. a) Calculated IR spectrum of *s-trans*-**4a** at the B3LYP/6-31G* level, b) Ar matrix IR spectrum (12 K) of *s-trans*-**4a** (positive peaks), obtained by subtracting the spectrum of the FVT of **3a** at 500 °C from the spectrum of **3a** itself (negative peaks). ■: peaks due to *s-cis*-**4a** (2134, see Figure 1a for details); 1233 cm^{-1}).

calculated for *s-trans*-**4a** shows that the ratios between the band at 2138 cm^{-1} and those in the fingerprint region are too small; the band at 2142 cm^{-1} is the only one in the C=C=O stretch region that agrees with the calculated ratio (of course, the errors in the calculated intensities are unknown, but they are not expected to be large). As it will be seen below, the band at

Table 1. IR data [a] for *s-trans*-**4a**, matrix isolated in argon at 12 K and calculated at the B3-LYP/6-31G* level.

Calculated $\tilde{\nu}$ [c]	I	Experiment [b] $\tilde{\nu}$	I [d]	Calculated $\tilde{\nu}$ [c]	I	Experiment [b] $\tilde{\nu}$	I [d]
748	89	766	s	1458	6	1453	vw
814	15	830	w	1478	11	1469	w
926	8	941	vw	1636	164	1646	s
1083	51	1088	m	2143	819	2142	vs
1096	32	1092	s	2916	36	2913	vw
1141	1	1167	vw	2974	40	2970	b
1185	11	1200	w	3039	18	3016	vw
1270	112	1273	s	3083	0		
1337	89	1347	m	3105	8		
1418	16	1399	w	3162	7	3122	vw
1448	5	1451	vw				

[a] Frequencies in cm^{-1} and intensities in $km\,mol^{-1}$. [b] *s-trans*-**4a** generated by FVT/matrix isolation (Ar, 12 K) of **3a**. [c] Scaled by 0.9613 (ref. [30]). [d] Relative intensity: vw = very weak, w = weak, m = medium, s = strong, vs = very strong, b = broad.

2138 cm^{-1} is assigned to a site of the *s-trans* form, and the one at 2134 cm^{-1} to the *s-cis* form. The corrected ratio[10] *s-cis*:*s-trans* is ca. 0.1:1.

Further evidence supporting the assignments is given by generation of these bands by Ar matrix photolysis (6.5 K) of **3a** (1000 W high-pressure Hg–Xe lamp; broad band; quartz). The *s-cis* form absorbing at 2134 cm^{-1} is generated first (the evidence for this is given by a comparison of calculation with experiment) (Figure 3 and Table 2), but isomerizes to the *s-trans*

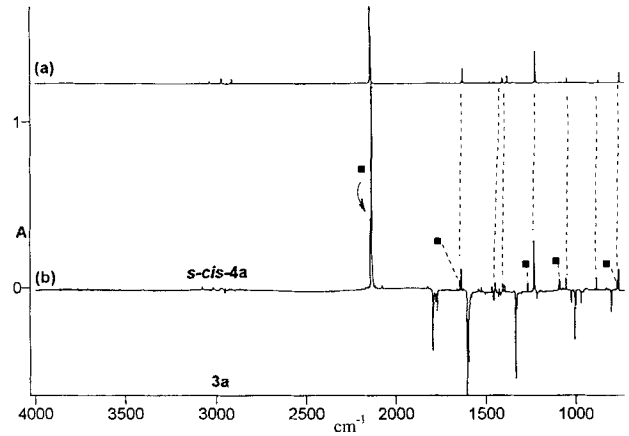

Figure 3. IR spectra of *s-cis*-**4a**. a) Calculated IR spectrum of *s-cis*-**4a** at the B3LYP/6-31G* level, b) Ar matrix IR spectrum (6 K) of *s-cis*-**4a** (positive peaks), obtained after subtracting the spectrum of the photolysis (broad band) of **3a** for 6 min from the spectrum of **3a** itself (negative peaks). ■: peaks due to *s-trans*-**4a** (2142, 2138 (see details in Figure 4a), 1646, 1272, 1092 cm^{-1}).

form (2142 and 2138 cm^{-1}) on further photolysis (ca. 1:1:2.5 ratio after 6 min changing to a ca. 1:1:1.2 ratio after 25 min, and finally to ca. 1:1:1 after 41 min). The nearly constant ratio between peaks at 2142 and 2138 cm^{-1} appears to confirm that both of these peaks belong to the *s-trans* form. Furthermore, when these two bands increase in intensity, the other peaks belonging to the *s-trans* form (cf. Figure 2) also increase in intensity. When **3a** is thermolyzed at roughly constant temperature but otherwise different conditions (defined in the caption of Figure 1), the ratios of these three bands can change radically,

0947-6539/97/0302-0238 $ 15.00+.25/0 Chem. Eur. J. 1997, 3, No. 2

Table 2. IR data [a] for *s-cis*-**4a**, matrix isolated in argon at 12 K and calculated at the B3-LYP/6-31G* level.

Calculated $\tilde{\nu}$ [c]	I	Experiment [b] $\tilde{\nu}$	I [d]	Calculated $\tilde{\nu}$ [c]	I	Experiment [b] $\tilde{\nu}$	I [d]
754	82	759	s	1458	6		
873	22	887	w	1478	12	1469	w
925	5			1628	116	1637	s
1051	39	1057	m	2141	723	2134	vs
1091	9			2914	37		
1141	1			2972	41	2967	b
1182	4			3037	22	3015	vw
1226	246	1233	s	3081	0		
1381	56	1398	w	3089	11	3076	vw
1408	44	1409	w	3159	7		
1449	8	1451	w				

[a] Frequencies in cm^{-1} and intensities in $km\,mol^{-1}$. [b] *s-cis*-**4a** generated by irradiation (broad band, Ar, 12 K) of **3a**. [c] Scaled by 0.9613 (ref. [30]). [d] Relative intensity: vw = very weak, w = weak, m = medium, s = strong, vs = very strong, b = broad.

suggesting that the band at 2138 cm^{-1} may be due to a site effect and the one at 2134 cm^{-1} has contributions from both a site of the *s-trans* and the *s-cis* form. Another possibility to consider is the formation of a rotamer of the *s-trans* form involving rotation of the methoxy group (Scheme 3). Indeed, the methyl group

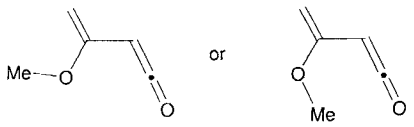

Scheme 3. Rotamers of *s-trans*-**4a**.

can be either proximal to or remote from the ketene moiety, and thus it can interact with this functionality, which is not possible in the *s-cis* form. Even though the value of 2138 cm^{-1} equals the wavenumber for CO in argon matrices,[11] this band cannot be due to CO formation because it is not observed when **3a** is thermolyzed between 400 and 650 °C and the products isolated neat at 12 K. Here, the ketenes give a single, unresolved band at 2129 cm^{-1}. Neat CO under these conditions absorbs at 2139 cm^{-1}. Likewise, it can be excluded that the band at 2142 cm^{-1} is due to the unsubstituted ketene itself, which could form in a cycloreversion of **3a** with concomitant formation of methoxyacetylene; no other bands that could be due to ketene[12] appear. Further evidence against this cycloreversion process is detailed below for the case of **3b**.

When the thermally and photochemically generated ketenes were trapped at −196 °C and subsequently warmed up, reversion to the starting material **3a** was observed at −15 °C. Although the *s-cis* species is formed first upon Ar matrix photolysis (12 K) after 5 min irradiation, the *s-trans* species is the only one observed on photolysis at 77 K, even after 5 min of irradiation. This observation as well as the higher proportion of the *s-trans* form on FVT can be understood in terms of a greater thermodynamic stability of the *s-trans* form and a low barrier for interconversion of the two isomers.[10b] To prove this, annealing experiments were carried out on the photochemically generated *s-cis* ketene in Xe matrix (10 K) (Figure 4). After 5 min of broad-band irradiation of **3a**, the *s-cis* and *s-trans* species were produced in a ca. 2.7:1 corrected ratio[10] (Figure 4, top). Annealing to 40 K did not modify this ratio. At 50 K, the 1234 cm^{-1} absorption characteristic of the *s-cis* form started to decrease slightly, with concomitant increase in the 1269 cm^{-1} band of the *s-trans* form. The corrected ratio was estimated to be 1.6:1. The small change observed at 50 K increased drastically with annealing at 60 K for 5 min. The *s-trans* species now became dominant, with a corrected ratio of 0.3:1. The conversion is so efficient that at 70 K only the *s-trans* form was observed after 5 min of annealing. In the C=C=O stretch region, too, a large change occurred. Before annealing, only two bands were observed at 2133 and 2130 cm^{-1} due to the *s-trans* and *s-cis* forms, respectively. After annealing to 70 K, three bands at 2133, 2130, and 2127 cm^{-1} were observed in this region, all belonging to the *s-trans* species, with a pattern similar to that found in Ar matrices (cf. Figure 1c–d).[10b]

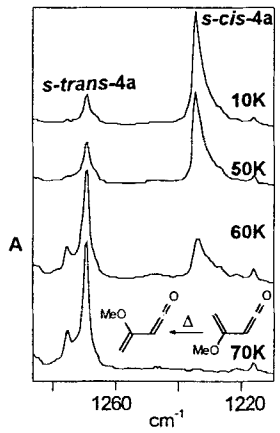

Figure 4. Annealing experiment of *s-cis*-**4a** in xenon matrix at different probe temperatures. The peaks characteristic of *s-cis*- and *s-trans*-**4a** are respectively 1234 (1226 calculated, Table 2) and 1269 cm^{-1} (1270.2 calculated, Table 1). *: site effect.

At FVT temperatures above 650 °C, weak allene bands were observed at 1980 and 1946 cm^{-1} (Ar, 12 K), increasing in intensity until ca. 900 °C (Figure 5a). Direct comparison with methyl allenecarboxylate (**5a**) confirmed the identity of these bands. The proof for the reversibility of this process was obtained when **5a** was thermolyzed at temperatures above 625 °C (Ar, 12 K). All the bands in the ketene region assigned to **4a** were also observed in the allene case (Figure 5b).

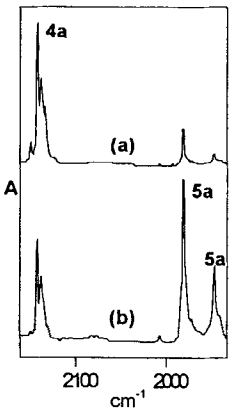

Figure 5. Partial Ar matrix FTIR spectra (12 K) of the results of FVT of a) **3a** at 700 °C; b) **5a** at 710 °C.

Analogous FVT/matrix isolation of 3-ethoxycyclobutenone[13] (**3b**) gave *s-cis*- and *s-trans*-ethoxyvinylketene (**4b**) above 400 °C. The conversion was complete at 700 °C. The characteristic IR bands of **4b** are at 2136 and 2140 cm^{-1} (Ar, 12 K). As in the previous case, the *s-trans* species at 2140 cm^{-1} is the main species formed on thermolysis. The evidence is again given by the very good agreement between calculation and experiment (Figure 6, Table 3). The *s-cis* conformer at 2136 cm^{-1} was observed as well in small quantity (ca. 0.1:1 ratio).[10a] Assuming this corrected ratio is accurate, then the measured ratio between the two peaks in the C=C=O stretch region is too small (0.7:1; the calculated extinction coefficients are roughly the same for these two peaks). This can again be understood if the peak at 2136 cm^{-1} is due to both a site of *s-trans*-**4b** and a contribution from *s-cis*-**4b**. This was confirmed by thermolysis of **3b** at 450 °C under different conditions. The peak at 2136 cm^{-1} decreased in intensity when the Ar dilution

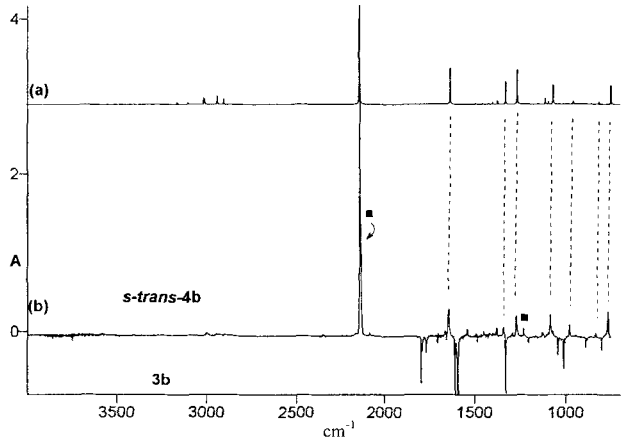

Figure 6. IR spectra of *s-trans*-**4b**. a) Calculated IR spectrum at the B3LYP/6-31G* level; b) Ar matrix spectrum (12 K) of *s-trans*-**4b** (positive peaks), obtained after subtracting the spectrum of the FVT of **3b** at 450 °C from the spectrum of **3b** itself (negative peaks). ■: *s-cis*-**4b** (2134, 1232 cm^{-1}).

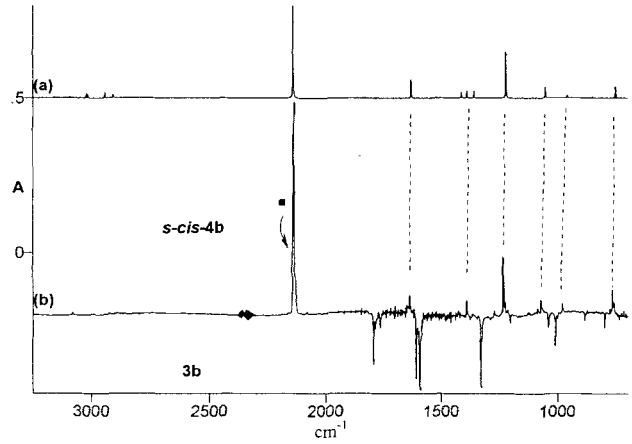

Figure 8. IR spectra of *s-cis*-**4b**. a) Calculated IR spectrum of *s-cis*-**4b** at the B3LYP/6-31G* level; b) Ar matrix spectrum (12 K) of *s-cis*-**4b** (positive peaks), obtained after subtracting the spectrum after photolysis (broad band) of **3b** for 5 min from the spectrum of **3b** itself (negative peaks). ■: *s-trans*-**4b** (2140 cm^{-1}; cf. Figure 7a).

Table 3. IR data [a] for *s-trans*-**4b**, matrix isolated in argon at 12 K and calculated at the B3-LYP/6-31G* level.

Calculated		Experiment [b]		Calculated		Experiment [b]	
$\tilde{\nu}$ [c]	*I*	$\tilde{\nu}$	*I* [d]	$\tilde{\nu}$ [c]	*I*	$\tilde{\nu}$	*I* [d]
748	87	765	m	1423	6		
812	0			1456	5	1449	vw
814	11	834	w	1472	3	1463	vw
919	1			1494	4	1487	vw
957	13	980	m	1634	168	1640,1644	s
1070	89	1086	m	2143	794	2140	vs
1095	13	1105	w	2905	23	2900	w
1112	27	1128	w	2941	34	2946	b
1151	5			2943	16		
1259	1			3011	22	3000	b
1267	156	1272	s	3017	29		
1329	105	1340	m	3082	0		
1373	16	1379	m	3104	8	3093	w
1400	9	1399	vw	3161	8		

[a] Frequencies in cm^{-1} and intensities in km mol^{-1}. [b] *s-trans*-**4b** generated by FVT/matrix isolation (Ar, 12 K) of **3b**. [c] Scaled by 0.9613 (ref. [30]). [d] Relative intensity: vw = very weak, w = weak, m = medium, s = strong, vs = very strong, b = broad.

Table 4. IR data [a] for *s-cis*-**4b**, matrix isolated in argon at 12 K and calculated at the B3-LYP/6-31G* level.

Calculated		Experiment [b]		Calculated		Experiment [b]	
$\tilde{\nu}$ [c]	*I*	$\tilde{\nu}$	*I* [d]	$\tilde{\nu}$ [c]	*I*	$\tilde{\nu}$	*I* [d]
754	79	766	m	1413	5		
814	0			1457	5		
853	9			1472	3		
912	2			1494	5		
960	16	980	m	1626	122	1633	s
1053	71	1071	m	2140	745	2134	vs
1091	8			2904	23		
1107	9	1128	w	2940	34	2932	vw
1151	4			2944	18	2945	vw
1221	311	1232	s	3012	24	3001	vw
1262	1			3018	30	3009	vw
1356	47	1365	vw	3080	0		
1386	47	1390	m	3089	10	3078	w
1409	37	1427	w	3159	8		

[a] Frequencies in cm^{-1} and intensities in km mol^{-1}. [b] *s-cis*-**4b** generated by irradiation (broad band, Ar, 12 K) of **3b**. [c] Scaled by 0.9613 (ref. [30]). [d] Relative intensity: vw = very weak, w = weak, m = medium, s = strong, vs = very strong, b = broad.

factor increased, that is, when the concentration of **3b** in the gas phase decreased. The *s-cis* form absorbing at 2136 cm^{-1} was generated first on Ar matrix photolysis of **3b** (broad band), but as expected isomerized to *s-trans*-**4b** (2140 cm^{-1}) on further irradiation (2.8:1 ratio after 5 min, changing to 0.8:1 after 30 min; Figure 7). Once again, the calculated and experimental IR spectra of *s-cis*-**4b** are in excellent agreement (Figure 8, Table 4).

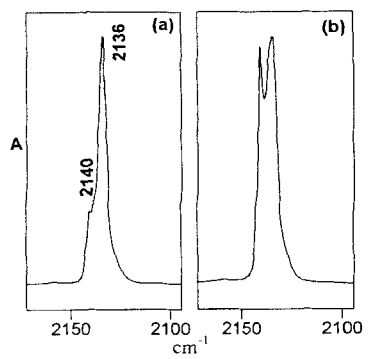

Figure 7. Partial Ar matrix FTIR spectra (6 K) of the results of photolysis (broad band) of **3b** after a) 5 min and b) 30 min. Peaks at 2136 and 2140 cm^{-1} are due to *s-cis*-**4b** and *s-trans*-**4b**, respectively.

It was mentioned above that **3a** did not decompose into ketene (**10**) and methoxyacetylene on FVT. Evidence is now given for the ethyl analogue **3b** (Scheme 4). Ethoxyacetylene (**9**) was prepared[14] and thermolyzed. On matrix isolation (Ar, 12 K), the characteristic absorptions of **9** are at 3351 (s) and 3346 (s) cm^{-1} for the CH stretch and 2180 (w), 2169 (vs), and 2156 (w) cm^{-1} for the CC stretch. None of the absorptions assigned to **9** or **10**[12] were observed on thermolysis of **3b** at 400–920 °C. FVT/matrix isolation of **9** gave **10** and ethene above 400 °C.[15] A six-electron transition state is postulated for this known process.[1a, 16]

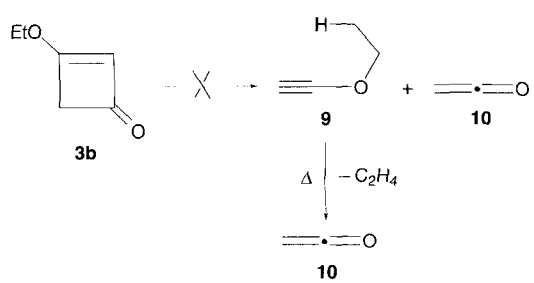

Scheme 4.

0947-6539/97/0302-0240 $ 15.00+.25/0 Chem. Eur. J. 1997, 3, No. 2

Formation of the starting material **3b** was observed when the thermally or photochemically generated ketenes **4b** were warmed from −196 °C to −25 °C. Interconversion of the less stable *s-cis* to the more stable *s-trans* form of **4b** was observed in annealing experiments in Xe matrix in analogy with Figure 4.

Chemical evidence for the structure of **4b** was obtained by generation at 450 °C with trapping on a cold finger coated with MeOH at −196 °C. After the finger had been allowed to warm up to room temperature, ^{1}H NMR analysis demonstrated the formation of methyl 3-ethoxy-3-butenoate (**6**) and methyl (*E*)-3-ethoxy-2-butenoate ((*E*)-**7**) in a ratio 64:36 (70% yield with 26% of **3b** recovered) (Scheme 5). Photolysis of **3b** on a preparative scale in methanol solution gave, after purification, **6** and (*E*)-**7** as a mixture as well as methyl (*Z*)-3-ethoxy-2-butenoate ((*Z*)-**7**) in a ratio 44:47:7 (80% yield with 2% of **3b** recovered).

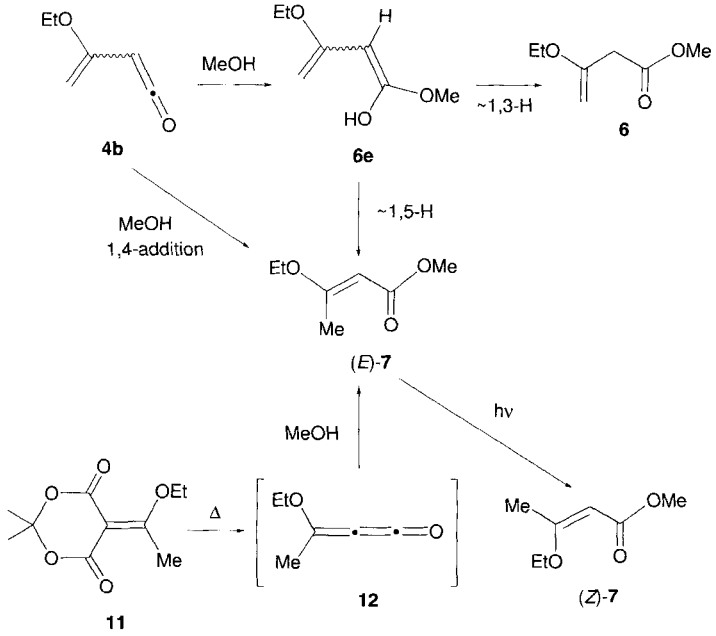

Scheme 5.

(*Z*)-**7** is formed by photochemical *cis–trans* isomerization of (*E*)-**7**. The formation of **6** and (*E*)-**7** can be understood in terms of initial formation of an enol **6e** (or enolate)[17] (Scheme 5). (*E*)-**7** may also be formed by 1,4-addition. Isomerization of the less stable β,γ-unsaturated ester[18] **6** to the α,β-conjugated ester (*E*)-**7** was not observed: GC-MS of the mixture of photochemically prepared **6** and (*E*)-**7**, with 60–100 °C as the initial temperature, gave no change in the ratio of these two compounds. Compound (*E*)-**7** was also obtained from ethoxymethyleneketene (**12**), itself prepared by FVT of the Meldrum's acid derivative **11** at 475 °C.[19]

FVT of **3b** above 690 °C gave rise to allene bands at 1985, 1979, and 1943 cm^{-1} (Ar, 12 K) or 1971 and 1941 cm^{-1} (neat, 77 K), identical with those of ethyl allenecarboxylate (**5b**). The latter was also unambiguously identified by ^{1}H NMR spectroscopy of the product of a preparative thermolysis of **3b** at 690 °C .

The allene bands in the IR spectrum increased until 730 °C, whereupon they decreased again, disappearing entirely at 920 °C. Throughout this temperature range (≈600–920 °C), a new set of bands belonging to acetylketene (**8**) grew in intensity.[20] As we have recently characterized acetylketene very thoroughly,[8] we readily recognized this pattern as the *s-trans* and *s-cis* forms of **8** (ratio ca. 1:1).[21] Bands due to ethene were also identified at 948, 2996, and 3096 cm^{-1}. The formation of acetylketene and ethene is readily understood in terms of thermal *cis*-elimination through a six-electron transition state from the ethoxyvinylketenes (**4b**) (Scheme 6).

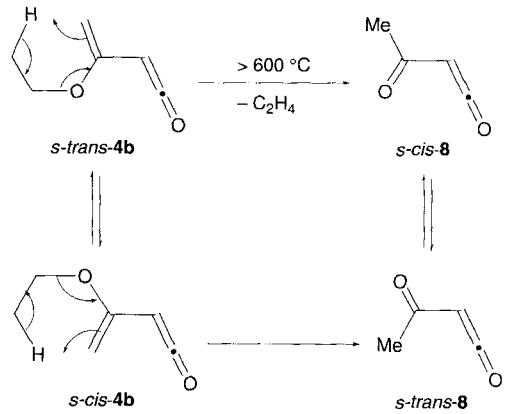

Scheme 6.

At still higher temperatures (>800 °C) acetylketene underwent partial decomposition to give CO_2 and propyne **15** (3323, 2137 cm^{-1}) (also observed when other acetylketene precursors[8] were used).[22]

Proof of the interconversion of vinylketenes **4b** and ethoxycarbonylallene **5b** was obtained by FVT of the latter at 570–800 °C. Again, the vinylketene bands due to *s-cis-* and *s-trans-***4b** were observed, as well as those due to *s-cis-* and s-*trans-***8** and ethene, which increased in intensity with the temperature. The formation of **8**, ethene, **15**, and CO_2 by FVT of **5b** was confirmed by direct on-line monitoring of the reactions by mass spectrometry.[23]

Another allene derivative was briefly investigated and indicates the generality of the rearrangement. Thus, FVT of trimethylsilyl allenecarboxylate (1972, 1942 cm^{-1}; 77 K) at temperatures above 600 °C gave rise to a ketene absorption at 2126 cm^{-1}.

2. Dimethylamino group: Probably the most intriguing 1,3-shift is that involving the amino group (Scheme 7). A variation of the method described by Wasserman et al. was used to prepare **3c**.[13]

FVT of **3c** caused the emergence of new allene absorptions due to **5c** at 1969 and 1948 cm^{-1} (77 K) already at 500 °C in agreement with the lower calculated barrier for the 1,3-shift of a dialkylamino group (see Section 4). Allene **5c** was unambiguously identified by direct comparison with an authentic sample, but **4c** was not observed at all on thermolysis, even when using matrix isolation (Ar, 12 K). It was, however, observed at 2132 cm^{-1} on broad-band photolysis of **3c** in an Ar matrix at 12 K.[24] The amount of ketene generated by photolysis of a film of neat **3c** at 77 K was, however, too small for a meaningful warmup experiment to determine wether this ketene cyclized back to **3c**.

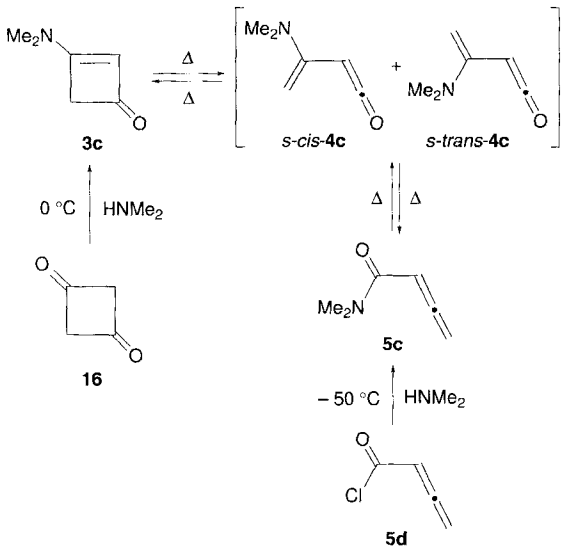

Scheme 7.

The 1,3-shift of the dimethylamino group was confirmed by FVT of allenic amide **5c**, obtained by adding 2,3-butadienoyl chloride (**5d**) to a solution of diethylamine in THF.[25] Even though **4c** itself was not observed, strong evidence was provided by the isolation of **3c** by using FVT temperatures above 470 °C. By Ar matrix isolation (12 K) **3c** was characterized at 1772, 1722, 1391, 1362, and 1038 cm^{-1}. At higher temperature **5c** decomposes further through a retroene reaction, which will be described elsewhere.[21b]

3. Chloro substituent: 2,3-Butadienoyl chloride (**5d**) was subjected to FVT between 320 and 850 °C. A ketene band was observed on argon matrix isolation (12 K) above 370 °C (Figure 9a) due to the exclusive formation of *s-trans*-(chlorovinyl)-

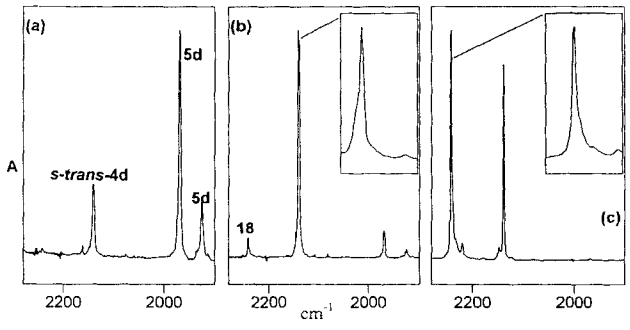

Figure 9. Partial Ar matrix FTIR spectra (12 K) of the results of FVT of **5d**, a) *s-trans*-**4d** (2140 cm^{-1}) formed at 400 °C, b) *s-trans*-**4d** (cf. Figure 10c, Table 5) at 530 °C, c) **18** (2242 cm^{-1}; cf. Table 6) and **4d** formed at 800 °C.

ketene (*s-trans*-**4d**, Scheme 8). The evidence is given by the very good agreement between calculated and experimental data (Figure 10b,c; Table 5). The *s-cis* rotamer was not observed: *s-cis*-**4d** has the strongest calculated absorption (in the fingerprint region) at 1087 cm^{-1} and no signal near this value was detectable (Figure 10a,c; Table 5).

Generation of **4d** at 550 °C with trapping on a cold finger coated with methanol at −196 °C gave mainly 3-chloro-3-butenoate[26] (**17**) (73% yield). Not even traces of 3-chloro-2-

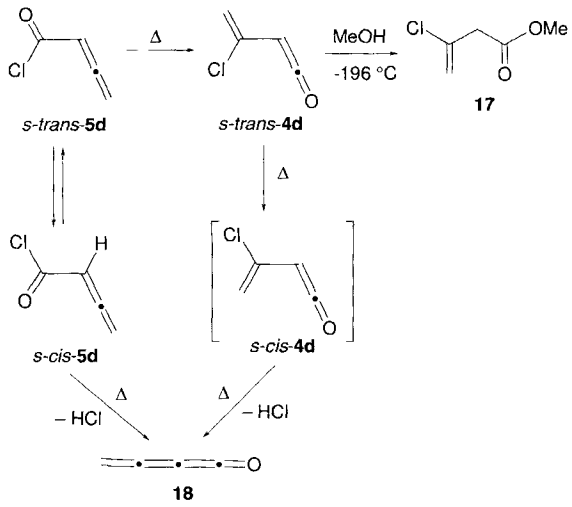

Scheme 8.

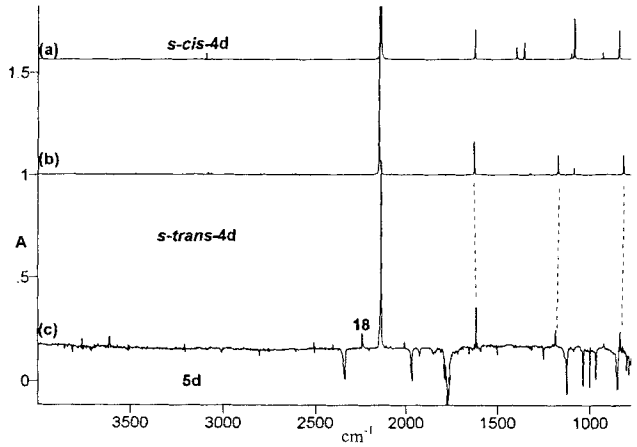

Figure 10. IR spectra of *s-trans*-**4d**. Calculated IR spectrum of a) *s-cis*-**4d** and b) *s-trans*-**4d** at the B3LYP/6-31G* level. c) Ar matrix spectrum of *s-trans*-**4d** (positive peaks), obtained after subtracting the spectrum of the FVT of **5d** at 530 °C (Figure 9b) from the spectrum of **5d** itself (negative peaks).

Table 5. IR data [a] for *s-trans*-**4d**, matrix isolated in argon and nitrogen at 12 K, and for *s-trans*- and *s-cis*-**4d**, calculated at the B3-LYP/6-31G* level.

s-trans-**4d**, calcd [b] $\tilde{\nu}$	*I*	*s-trans*-**4d**, Ar [c] $\tilde{\nu}$	*I* [d]	*s-trans*-**4d**, N_2 [c] $\tilde{\nu}$	*I* [d]	*s-cis*-**4d**, calcd [b] $\tilde{\nu}$	*I*
817	601	835	m	847, 844	m	842	56
907	9	924	w			931	12
1090	20					*1087*	*80*
1175	62	1188	m	1191	m	1103	11
1326	3					*1359*	*32*
1417	3					1399	22
1628	106	1616	s	1616	s	1625	58
2149	838	2140	vs	2144	vs	2141	740
3064	3					3062	1
3079	7					3091	12
3155	2					3151	1

[a] Frequencies in cm^{-1} and intensities in $km\,mol^{-1}$. [b] Frequencies scaled by 0.9613 (ref. [30]). [c] *s-trans*-**4d** generated by FVT/matrix isolation (Ar or N_2, 12 K) of **5d**. [d] Relative intensity: vw = very weak, w = weak, m = medium, s = strong, vs = very strong, b = broad.

butenoate[27] were detected. When the thermally generated ketene **4d** (2130 cm^{-1}, 77 K) was warmed from −196 °C to −25 °C in an Ar atmosphere, several new bands in the carbonyl region were observed, but no major compound could be

0947-6539/97/0302-0242 $ 15.00+.25/0 Chem. Eur. J. 1997, 3, No. 2

isolated. 3-Chlorocyclobutenone is less stable than ketene **4d**.[28]

FVT above 530 °C (Figure 9b) gave rise to a new band at 2242 cm^{-1} due to the formation of butatrienone (**18**) and HCl (2888, 2864, and 2816 (dimer) cm^{-1}). This band became dominant at above 780 °C (Figure 9c). This latter observation is in agreement with a report by Brown et al.,[24] who observed **18** on FVT of **5d** between 710–880 °C. A comparison with the data of Brown et al., and with calculations, shows very good agreement (Table 6; Figure 9b–c).

Table 6. IR data [a] for butatrienone (**18**), matrix isolated in argon at 12 K and calculated at the B3-LYP/6-31G* level

Calculated [b]		Experiment [c]		Literature [d]	
$\tilde{\nu}$	I	$\tilde{\nu}$	I [e]	$\tilde{\nu}$	I
		1454	m	1456	11
1484	82	1495	m	1495	6
2003	1				
		2220	s	2219	26
2267	1976	2242	vs	2242	88
		2965	w	2964	1
3044	13	3025	w	3025	3
3117	1				

[a] Frequencies in cm^{-1} and intensities in km mol^{-1}. [b] Frequencies scaled by 0.9613 (ref. [30]). [c] **18** generated by FVT/matrix isolation (Ar, 12 K) of **5d**. [d] R. F. C. Brown et al. (ref. [24]). [e] Relative intensity: w = weak, m = medium, s = strong, vs = very strong.

One source of **18** could be *syn*-elimination of HCl from *s-cis*-**5d**. Another pathway would be the HCl elimination from *s-cis*-**4d** itself (Scheme 8). The fact that the *s-cis* form of **4d** is not observed is probably due to stability differences. According to calculations (cf. Section 4) *s-trans*-**4d** is predicted to be more stable than the *s-cis* form by 9 kJ mol^{-1} with a rotation barrier of 19 kJ mol^{-1}.

4. Theory: The structures and energies of vinylketenes **19** and acylallenes **20**, and transition structures for the 1,3-R migration (**21**) (Scheme 9), were investigated using the G2(MP2,SVP) theory.[29] Note that the calculated G2(MP2,SVP) relative energies are close to those reported earlier at the QCISD(T)/6-311+G(2d,p)//MP2/6-31G*+ZPVE level.[6] Optimized structural parameters for *s-trans*-**19**, *s-trans*-**20**, and the **21** are given

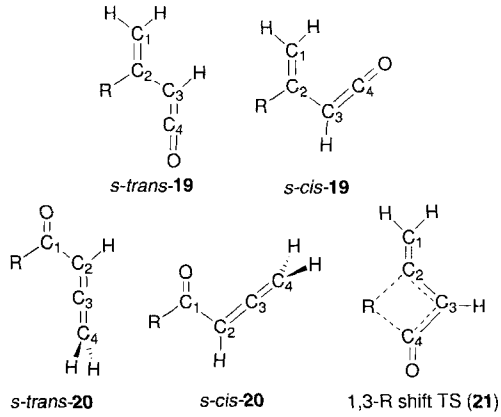

Scheme 9. R = H (**a**), CH_3 (**b**), NH_2 (**c**), OH (**d**), F (**e**), SH (**f**), Cl (**g**), OCH_3 (**h**), SCH_3 (**i**), and $N(CH_3)_2$ (**j**).

Table 7. Calculated structural parameters (MP2/6-31G*) [a] for *s-trans*-**19**, *s-trans*-**20**, and **21** [b].

	H	CH_3	NH_2	OH	F	SH	Cl	OCH_3	SCH_3	$N(CH_3)_2$
s-trans-**19**										
$r(R-C_2)$	1.089	1.506	1.414	1.388	1.367	1.780	1.749	1.373	1.773	1.421
$r(C_1-C_2)$	1.344	1.346	1.347	1.344	1.336	1.347	1.342	1.347	1.349	1.349
$r(C_2-C_3)$	1.458	1.465	1.466	1.456	1.451	1.461	1.454	1.460	1.464	1.469
$r(C_3-C_4)$	1.329	1.329	1.331	1.330	1.331	1.330	1.332	1.329	1.330	1.331
$r(C_4-O)$	1.181	1.181	1.180	1.178	1.177	1.179	1.177	1.179	1.180	1.180
$\sphericalangle RC_2C_1$	119.3	122.1	124.0	124.3	119.7	123.8	119.9	126.1	125.2	124.9
$\sphericalangle RC_2C_3$	116.8	117.2	113.2	110.7	111.8	114.6	115.3	109.9	114.0	113.3
$\sphericalangle C_2C_3C_4$	122.3	122.6	120.7	120.6	120.0	124.2	122.9	120.5	124.5	119.8
s-trans-**20**										
$r(R-C_1)$	1.108	1.512	1.369	1.360	1.364	1.801	1.791	1.354	1.785	1.370
$r(C_1-O)$	1.227	1.231	1.231	1.221	1.202	1.222	1.207	1.222	1.227	1.237
$r(C_1-C_2)$	1.475	1.487	1.496	1.477	1.470	1.481	1.472	1.480	1.482	1.499
$r(C_2-C_3)$	1.321	1.320	1.317	1.318	1.319	1.318	1.319	1.318	1.318	1.317
$r(C_3-C_4)$	1.311	1.312	1.313	1.310	1.309	1.311	1.309	1.310	1.311	1.313
$\sphericalangle RC_1O$	121.6	122.2	123.1	123.0	121.1	122.5	120.7	124.0	122.3	123.1
$\sphericalangle RC_1C_2$	115.2	118.3	116.0	113.0	112.2	115.5	115.1	112.4	116.2	118.6
$\sphericalangle C_1C_2C_3$	120.1	123.3	124.0	123.3	122.4	123.3	124.3	123.5	123.6	124.2
TS **21**										
$r(R-C_2)$	1.438	2.012	1.906	1.811	1.799	2.197	2.229	1.802	2.178	1.968
$r(R-C_4)$	1.421	1.967	1.519	1.595	1.712	2.019	2.226	1.579	1.937	1.507
$r(C_1-C_2)$	1.337	1.331	1.328	1.325	1.317	1.329	1.321	1.327	1.331	1.329
$r(C_2-C_3)$	1.381	1.370	1.375	1.374	1.370	1.376	1.367	1.373	1.378	1.369
$r(C_3-C_4)$	1.414	1.396	1.424	1.408	1.393	1.415	1.395	1.410	1.422	1.428
$r(C_4-O)$	1.201	1.198	1.218	1.198	1.177	1.201	1.177	1.200	1.210	1.221
$\sphericalangle RC_2C_1$	123.1	113.5	122.3	117.5	114.9	123.0	117.9	117.4	123.4	122.4
$\sphericalangle RC_2C_3$	85.9	96.4	81.9	85.1	87.3	88.0	91.9	85.0	86.8	80.9
$\sphericalangle C_2C_3C_4$	95.7	101.0	102.2	101.8	104.8	109.4	113.0	101.2	107.3	102.8
$\sphericalangle C_3C_4O$	146.4	144.5	140.0	146.1	152.5	140.7	150.0	145.9	139.7	138.9

[a] Bond lengths in Å and bond angles in degrees. [b] Atom labels are given in Scheme 9.

Table 8. Calculated relative energies (kJ mol^{-1}) [a,b].

R	*s-trans*-**19**	*s-cis*-**19**	*s-trans*-**20**	*s-cis*-**20**	**21**
H (**a**)	0.0	6.0	44.7	56.6	272.5
CH_3 (**b**)	0.0	8.2	32.9	41.8	332.6
NH_2 (**c**)	0.0	3.5	−22.3	−13.1	165.7
OH (**d**)	0.0	8.5	−24.6	−23.0	186.1
F (**e**)	0.0	6.1	−17.2	−15.0	184.0
SH (**f**)	0.0	4.3	8.7	14.7	152.7
Cl (**g**)	0.0	8.7	11.8	16.0	156.9
OCH_3 (**h**)	0.0	8.2	−23.6	−23.0	169.0
SCH_3 (**i**)	0.0	4.5	4.6	8.3	146.7
$N(CH_3)_2$ (**j**)	0.0	2.3	−13.2	−9.9	128.8

[a] G2(MP2,SVP) E_0 values. [b] Calculated E_0 values for *s-trans*-**19** (G2(MP2,SVP)): −229.60378 (R = H), −268.64766 (R = CH_3), −284.68675 (R = NH_2), −304.55127 (R = OH), −328.56117 (R = F), −627.14902 (R = SH), −688.54812 (R = Cl), −343.72770 (R = OCH_3), and −666.33799 (R = SCH_3), and −363.05063 (R = $N(CH_3)_2$) hartrees.

in Table 7 and calculated G2(MP2,SVP) relatives energies are summarized in Table 8.

Vinylketene/acylallene equilibrium: There are two possible conformations of vinylketenes **19** and acylallenes **20**, *s-trans* and *s-cis* (Scheme 9). For all the substituents considered (**a**–**j**), the *s-trans* conformation is the preferred conformer (Table 8). The *s-cis*/*s-trans* energy difference ranges from 2 to 12 kJ mol^{-1}. The *s-trans* and *s-cis* conformers are connected by the transition structure for rotation. The calculated rotational barriers for vinylketenes are of the order of 20 kJ mol^{-1} (R = H, Cl, and OCH_3). A slightly higher value, 31 kJ mol^{-1} for R = H, is predicted for the rotational barrier for acylallenes. Thus, one would

expect the two conformers of vinylketenes and acylallenes to exist in equilibrium under high-temperature FVT conditions. This result is consistent with the experimental observations of both conformers for methoxy- and ethoxy-substituted vinylketenes. The calculated vinylketene/acylallene energy difference depends on the R substituent. A greater stability of the allenes is predicted for R = NH_2, OH, F, OCH_3, and $N(CH_3)_2$, while vinylketenes are preferred for the others (Table 8).

Infrared Spectra: To facilitate the experimental characterization, infrared spectra of all ten vinylketenes **19** and acylallenes **20**, calculated at the B3-LYP/6-31G* level, are reported (Table 9). This level of theory is shown to provide reliable prediction for experimental frequencies.[30] For instance, the calculated (scaled) B3-LYP/6-31G* C=C=O frequencies of *s*-(*Z*)- and *s*-(*E*)-acetylketenes are 2150 and 2135 cm^{-1}, in excellent agreement with the experimental values (2143 and 2133 cm^{-1}, respectively).[8] The characteristic features of the IR spectra of the vinylketenes (**19**) are the strong absorption bands due to the ketenic (C=C=O) and ethylenic (C=C) stretching vibrations. In general, the *s-trans* conformers are calculated to have higher frequency and more intense ketenic and ethylenic stretching vibrations than the corresponding *s-cis* rotamers. The characteristic IR absorptions for acylallenes **20** are the allenic (C=C=C) and carbonyl (C=O) stretching vibrations. Here, the *s-cis* conformers are predicted to have higher frequency but less intense carbonyl bands than the corresponding *s-trans* forms. On the other hand, the *s-cis* conformers are calculated to have higher frequencies and more intense allenic bands. Thus, one may distinguish between the *s-trans* and *s-cis* conformers of vinylketenes and acylallenes based on the frequency difference and intensity ratio for their two characteristic vibrational modes. For *s-trans*- and *s-cis*-methoxyvinylketenes (**19d**, R = OCH_3), our calculated results for the C=C and C=C=O vibrations are in excellent accord with the observed values (Section 1; Figures 2, 3, 6, and 8).

Table 9. Calculated (B3-LYP/6-31G*) frequencies [a] (cm^{-1}) and infrared intensities (in parentheses, km mol^{-1}) of the main bands of vinylketenes **19** and acylallenes **20**.

R	*s-trans*-**19**	*s-cis*-**19**	*s-trans*-**20**	*s-cis*-**20**
H	2133 (899)	2128 (698)	1968 (108)	1971 (141)
	1637 (68)	1634 (42)	1727 (310)	1726 (186)
CH_3	2129 (807)	2129 (716)	1971 (103)	1975 (153)
	1639 (56)	1642 (34)	1714 (251)	1721 (141)
NH_2	2133 (781)	2138 (691)	1974 (80)	1988 (110)
	1653 (121)	1644 (105)	1726 (361)	1727 (227)
OH	2146 (838)	2143 (691)	1982 (109)	1987 (120)
	1651 (212)	1641 (151)	1754 (405)	1759 (246)
F	2152 (863)	2147 (682)	1981 (104)	1983 (114)
	1670 (177)	1661 (118)	1819 (427)	1822 (269)
SH	2138 (793)	2136 (768)	1975 (85)	1976 (163)
	1605 (78)	1606 (43)	1717 (322)	1732 (191)
Cl	2149 (838)	2141 (740)	1979 (98)	1973 (156)
	1628 (106)	1625 (58)	1791 (394)	1805 (233)
OCH_3	2143 (819)	2141 (723)	1982 (110)	1986 (122)
	1636 (164)	1628 (116)	1735 (313)	1741 (181)
$N(CH_3)_2$	2131 (745)	2135 (748)	1978 (77)	1985 (129)
	1619 (114)	1609 (107)	1674 (347)	1677 (230)
SCH_3	2136 (787)	2134 (797)	1975 (92)	1976 (166)
	1598 (74)	1599 (52)	1690 (268)	1705 (156)

[a] Scaled by 0.9613 (ref. [30]).

1,3-Migration: As with α-oxoketenes[3] and imidoylketenes,[5] the concerted 1,3-R shift, via a four-centered transition structure **21**, is the most favorable route for 1,3-migration in vinylketenes. Other plausible routes for the 1,3-migration process, namely, cleavage of the C–R bond and recombination, and two successive 1,2-R shifts, are calculated to be higher in energy (by 444 and 395 kJ mol^{-1}, respectively, for R = H). The direct 1,3-hydrogen shift of the parent compound (**19a**) requires an activation barrier of 273 kJ mol^{-1}. This is significantly higher than those calculated for the oxo (143 kJ mol^{-1}) and imine (194 kJ mol^{-1}) analogues.

Next, we consider the effect of several simple substituents—CH_3 (**b**), NH_2 (**c**), OH (**d**), F (**e**), SH (**f**) and Cl (**g**)—on the calculated 1,3-migration barrier height. As shown in Table 8, substitution of an electron-rich group (**c**–**g**), with one or more unshared pairs of electrons, for hydrogen decreases the activation barrier. On the other hand, a significant destabilizing effect is calculated for a methyl substituent (**b**). As with α-oxoketenes and imidoylketenes, the origin of the dramatic rate acceleration by electron-rich substituents in vinylketene–acylallene rearrangements can be understood in terms of a favorable donor–acceptor interaction. The direct 1,3-R shift involves an interaction between the R group and the central carbon atom of the ketene moiety in the four-centered transition structure. The lowest unoccupied molecular orbital (LUMO) of *s-trans*-vinylketenes (or acylallenes) indicates that there is a vacant atomic p orbital (with the largest coefficient) at the central carbon atom in the molecular plane (Figure 11a). Thus, one would expect n electron donor substituents (**c**–**g**) to interact favorably with the vacant p orbital and thus stabilize the 1,3-migration transition structures. The (symmetry allowed) donor–acceptor interaction between the lone pair electrons of a hydroxyl group and the ketene acceptor orbital in **19d** is illustrated in Figure 11b.

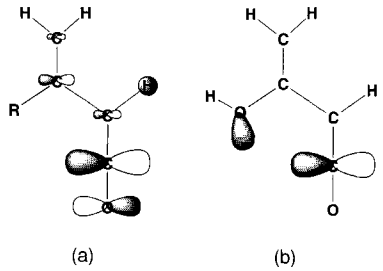

Figure 11. a) The lowest unoccupied molecular orbital (LUMO) of *s-trans*-vinylketenes. b) The donor–acceptor interaction between the lone pair electrons of a hydroxyl group and the vacant carbon p orbital of the ketene in **19d**.

For the second-row substituents, SH (**f**) and Cl (**g**), the calculated barriers are lower, by ≈30 kJ mol^{-1}, than those of the corresponding first-row analogues (i.e., OH (**d**) and F (**e**), respectively). The lower activation barriers may partly be attributed to the fact that the four-centered transition structures in the second-row systems (**21f** and **21g**) have significantly less ring strain. This is reflected in the larger calculated $C_2C_3C_4$ bond angles for transition structures **21f** and **21g** (Table 7). The 1,3-shift transition structure (**21**) involve a partially broken C_2–R bond. Thus, the magnitude of the C–R bond dissociation energy, which is smaller for the second-row systems, could also be a

0947-6539/97/0302-0244 $ 15.00+.25/0 Chem. Eur. J. 1997, 3, No. 2

contributing factor influencing the barrier height. Second-row elements are less electronegative and more nucleophilic. They are "soft" nucleophiles in the sense of hard and soft acids and bases. The methyl group (**b**) is calculated to be a poor migrator. In this case, there is no lone pair available for a donor–acceptor interaction. Furthermore, a pentacoordinated carbon is required in the 1,3-migration transition structure (**21b**). As a consequence, the 1,3-methyl shift in vinylketene would involve a very substantial barrier of 333 kJ mol^{-1}, 60 kJ mol^{-1} higher than the 1,3-hydrogen shift in **19a**.

The importance of donor–acceptor interaction is further supported by calculations on methyl-substituted n electron donor groups, namely, OCH_3 (**h**), SCH_3 (**i**), and $N(CH_3)_3$ (**j**). Methyl substitution on OH (**d**), NH_2 (**c**), and SH (**f**) groups increase their electron-releasing abilities, and thus one would expect an increase in strength of the donor–acceptor interaction. Indeed, the calculated barrier heights for OCH_3, SCH_3, and $N(CH_3)_2$ substituents are significantly less than for the corresponding unsubstituted ones (i.e., OH, SH, and NH_2, respectively), by 17, 6, and 37 kJ mol^{-1}, respectively. Thus, the predicted order of 1,3-migratory aptitude in vinylketenes is $NR'_2 > SR' > OR'$, where R′ = alkyl group. This calculated trend agrees well with experimental findings for the 1,3-migration in imidoylketenes[4] and thioacyl isocyanates (R-C(=S)-N=C=O), isoelectronic analogues of acyl(vinyl)ketenes.[31] Our calculated activation energies for methoxy (**h**) and dimethylamino (**j**) substituents are 169 and 129 kJ mol^{-1}, respectively. These results are in excellent accord with experimental findings (Sections 1 and 2): the 1,3-migration process for **19j** requires a lower FVT temperature than that of **19h**. It is interesting to note that a stable cyclic intermediate (**22**) is calculated for the dimethylamino substituent. This intramolecular amine–ketene zwitterion lies 21 kJ mol^{-1} above the open-chain vinylketene (**19j**). However, ring-opening of this cyclic ylide to **19j** is associated with a small barrier of just 1 kJ mol^{-1}. The C–N bond distance is rather long (1.774 Å, MP2/6-31G*).

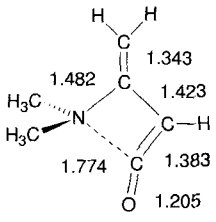

22

For all the R substitutents (**a**–**j**), the 1,3-migration barriers are in the order α-oxoketene < imidoylketene < vinylketene. In particular, the 1,3-migration barrier in vinylketene is approximately 100 kJ mol^{-1} higher than that of α-oxoketene. Thus, one can only expect to observe the vinylketene–acylallene rearrangement (**19**⇌**20**) for the most favorable migrating groups, that is, for alkoxy, thioalkoxy, amino groups, and the halogens. For 1,3-H migration, the calculated activation barrier increases along the series (H-C(=X)-CH=C=Y) α-oxoketene < α-oxoketenimine < imidoylketene < acylallene < vinylketene. An excellent correlation ($R^2 = 0.99$) is observed between the barrier height and the energy difference between the ketene LUMO (acceptor MO) and the occupied orbital (donor MO) involving the migrating group (Figure 12). This result provides further evidence for our donor–acceptor hypothesis.

In summary, electron-rich substituents strongly stabilize the transition structures for 1,3-migration in vinylketenes. The interaction between the R group and the ketene LUMO, in particular the atomic p orbital at the central carbon (Figure 11),

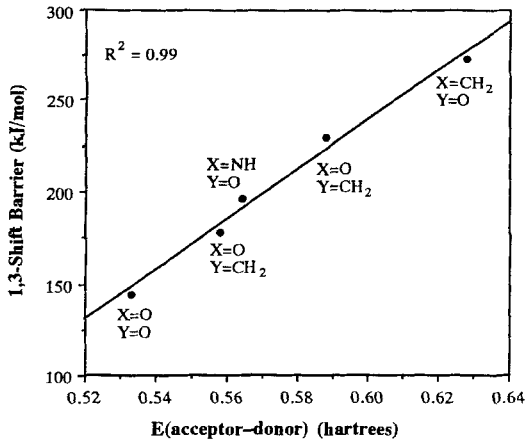

Figure 12. Plot of the 1,3-H shift barrier height (kJ mol^{-1}) against the energy difference (hartrees) between the orbitals of the donor (involving the migrating H atom) and the acceptor (ketene LUMO) for the series of cumulenes H-C(=X)-CH=C=Y (1 hartree = 2625.5 kJ mol^{-1}).

is the key factor in determining the magnitude of the activation barrier. The predicted migratory aptitude is in the order $N(CH_3)_2 > SCH_3 > SH > Cl > NH_2 > OCH_3 > OH > F > H > CH_3$. Since the methylthio group (**19i**) has an activation barrier (147 kJ mol^{-1}) smaller than that of the methoxy group (**19d**), we expect 1,3-*S*-alkyl shifts in (alkylthio)vinylketenes and -acylallenes[32] to be observable processes.

Conclusions

Alkoxyvinylketenes (**4a** and **4b**) undergo thermal interconversion with alkoxycarbonylallenes under FVT conditions above 630 °C, the allenes being the thermodynamically most stable isomers in this equilibrium. Allenecarboxamides isomerize to 3-aminocyclobutenone (**3c**) via unobserved aminovinylketenes **4c** above 500 °C. Chlorocarbonylallene **5d** interconverts with chlorovinylketene **4d** above 370 °C. A competing HCl elimination to butatrienone (**18**) is also observed. Ab initio calculations indicate that the vinylketene–acylallene rearrangements proceed via a concerted 1,3-R shift, involving a four-centered cyclic transition structure. The migratory aptitude is in the order $N(CH_3)_2 > SCH_3 > SH > Cl > NH_2 > OCH_3 > OH > F > H > CH_3$. The calculated barriers in the series R-C(=CH_2)-CH=C=O decrease with the increasing electron releasing ability of R. The stabilizing effect of the electron-rich substituents is readily understood in terms of the favorable interaction between the R group and the vacant central carbon p orbital of the ketene (or allene) moiety in the molecular plane.

Experimental and Computational Procedures

Computational Methods: Standard ab initio [33] and density functional [34] calculations were carried out with the Gaussian 92/DFT [35] system of programs. The structures and energies of vinylketenes, acylallenes, 1,3-migration transition structures, and related species were investigated by the G2(MP2,SVP) theory [29]. The G2(MP2,SVP) method, described in detail elsewhere [29], is a composite procedure based effectively on QCISD(T)/6-311+G(3df,2p)//MP2/6-31G* energies (evaluated by making certain additivity assumptions) together with zero-point vibrational and isogyric correc-

tions. Harmonic vibrational frequencies and infrared intensities were calculated at the B3-LYP/6-31G* level. The B3-LYP formulation [36] of density functional theory correspond to Becke's 3-parameter exchange functional [36a] together with Lee–Yang–Parr correctional functional [36b]. The directly calculated frequencies were scaled by 0.9613 to account for the average overestimation of vibrational frequencies at this level of theory [30]. The frozen-core approximation was employed for all single-point correlated calculations. All transition structures are calculated to have one imaginary frequency and the specific reactant and product linked by a particular transition structure were confirmed by intrinsic reaction coordinate (IRC) calculations.

Preparative flash vacuum thermolysis (FVT) was carried out in electrically heated quartz tubes, 40 cm long, 2 cm in diameter. Samples were sublimed or vaporized into the pyrolysis tube from a reservoir cooled in dichloromethane/liquid N_2, when necessary. The system was evacuated to ca. 10^{-5} mbar and continuously pumped during FVT using a Leybold-Heraeus turbomolecular pump PT 150. The pyrolysate was co-condensed with methanol vapor on the 77 K cold finger, whereby methanol was introduced between the exit of the pyrolysis oven and the cold finger. Further details of the FVT apparatus have been published [37].

Matrix isolation was carried out using 10 cm long, 0.8 cm diameter quartz tube in an oven directly attached to the vacuum shroud of a Leybold-Heraeus or Air Products liquid He cryostat [37]. Argon, nitrogen, and xenon were used as matrix media, which were passed over the sample while it was subliming and co-condensed as a matrix at ca. 12 or 6.5 K on a BaF_2 window for IR spectroscopy. Annealing experiments were carried out using a Lakeshore Model 330 autotuning temperature controller. Neat isolation at 77 K was carried out in a similar apparatus using a liq. N_2 cryostat [37].

Photolysis was carried out in quartz tubes (4.5 cm diameter, 20 cm length) using broad-band irradiation (1000 W high-pressure Hg–Xe lamps, Oriel).

Matrix IR spectra were recorded on Perkin Elmer 1720X or System 2000 instruments. ^1H and ^{13}C NMR spectra were recorded on a Bruker AC200 (200 MHz), mass spectra (70 eV; direct insertion) on a Kratos MS25RFA, and GC-MS on a Hewlett-Packard 5992B instrument.

Materials: Methyl(triphenylphosphoranylidene)acetate and ethyl (triphenylphosphoranylidene) acetate were obtained from Aldrich. Ketene [38] was produced using the ketene lamp described by Hurd and Williams [39]. Melting points are uncorrected.

3-Methoxycyclobutenone (3a) was synthesized according to ref. [7]. IR (neat, −196 °C): $\tilde{\nu}$ = 2945 (vw), 1775 (w), 1751 (m), 1654 (vw), 1584 (s), 1458 (w), 1433 (w), 1417 (w), 1341 (m), 1226 (w), 1043 (w), 1007 (m), 958 (m), 811 (w), 762 (w) cm^{-1}. IR (Ar matrix, 6 K): $\tilde{\nu}$ = 2994 (vw), 2983 (vw), 2950 (vw), 2897 (vw), 2842 (vw), 1793 (s), 1784 (w), 1778 (w), 1769 (m), 1600 (s), 1592 (s), 1461 (w), 1456 (w), 1434 (w), 1423 (w), 1334 (s), 1219 (w), 1028 (w), 1005 (s), 973 (m), 961 (m), 799 (m) cm^{-1}.

Methyl allenecarboxylate (5a): The procedure was modified from Hamlet and Barker [40]. Methyl(triphenylphosphoranylidene)acetate (4 g, 1.2×10^{-2} mol) was dissolved in dry dichloromethane (80 mL) containing hydroquinone (≈50 mg), and the solution was blanketed with an atmosphere of nitrogen. Into this solution, ketene [39,40], which was generated at a steady rate (≈0.35 mol h^{-1}), was introduced at 0 °C. When the reaction was complete (as shown by IR spectroscopy), the solvent was evaporated and petroleum ether (50 mL) was added. Triphenylphosphine oxide was filtered. After evaporation of the solvent, **5a** was distilled under vacuum as a clear liquid, b.p. 38–41 °C/13 mm Hg (lit. 40 °C/14 torr [41]); yield 35%. NMR data are in good agreement with ref. [41]. IR (neat, −196 °C): $\tilde{\nu}$ = 3064 (w), 3032 (w), 2990 (w), 2953 (w), 1971 (w), 1943 (w), 1714 (s), 1439 (w), 1347 (w), 1305 (w), 1267 (m), 1199 (m), 1173 (m), 1081 (w), 1027 (w), 861 (w), 780 (w) cm^{-1}. IR (Ar, 12 K): $\tilde{\nu}$ = 3034 (w), 3006 (w), 2962 (w), 2909 (vw), 2851 (vw), 2848 (vw), 1980 (m), 1946 (m), 1745 (m), 1740 (s), 1462 (w), 1441 (m), 1422 (w), 1361 (w), 1350 (w), 1334 (w), 1324 (w), 1300 (w), 1281 (w), 1267 (s), 1195 (m), 1167 (s), 1079 (w), 1046 (w), 1039 (w), 992 (w), 866 (w), 858 (w), 852 (w), 845 (w), 841 (w), 778 (w) cm^{-1}.

3-Ethoxycyclobutenone (3b) was synthesized according to the procedure of Wasserman et al. [13]. IR (neat, −196 °C): $\tilde{\nu}$ = 2985 (vw), 1782 (w), 1748 (w), 1577 (s), 1473 (w), 1448 (w), 1420 (w), 1400 (w), 1369 (w), 1329 (m), 1215 (w), 1158 (vw), 1078 (w), 1042 (vw), 1016 (m), 870 (m), 828 (w), 807 (m) cm^{-1}. IR (Ar matrix, 12 K): $\tilde{\nu}$ = 3005 (vw), 2956 (vw), 2950 (vw), 2909 (vw), 1790 (s), 1783 (m), 1761 (m), 1604 (s), 1588 (s), 1481 (w), 1425 (w), 1402 (vw), 1397 (vw), 1375 (w), 1327 (s), 1203 (w), 1040 (m), 1023 (w), 1008 (m), 1001 (w), 885 (w), 798 (m) cm^{-1}.

Trapping of Ketene 4b with Methanol:

Method A (flash vacuum thermolysis (FVT) of **3b**): **3b** (100 mg) was vaporized at 0 °C (5×10^{-5} mbar) and thermolyzed at 450 °C in the preparative FVT apparatus, with methanol as a trapping agent. Column chromatography ($SiO_2/CHCl_3$) of the crude product gave a mixture of **6** and (*E*)-**7** in a ratio 64:36 (85 mg, 70% yield) and **3b** (26%).

Method B (photolysis of **3b**): **3b** (100 mg, 8.93×10^{-4} mol) was added to dry methanol (100 mL) in a quartz tube. After degassing, the solution was irradiated with an aged broad-band lamp for 3 h. The reaction was monitored by TLC (SiO_2, $CHCl_3$). Column chromatography of the crude product gave a mixture of **6** and (*E*)-**7** in a ratio 49:51 (93 mg, 72%) and (*Z*)-**7** (8 mg, 7%). Data are reported below.

Methyl 3-ethoxy-3-butenoate (6): ^1H NMR (200 MHz, $CDCl_3$): δ = 4.05 (d, ^2J(H,H) = 2.2 Hz, 1H; (*Z*)-H4), 4.02 (d, ^2J(H,H) = 2.2 Hz, 1H; (*E*)-H4), 3.76 (q, ^3J(H,H) = 7 Hz, 2H; OCH_2), 3.71 (s, 3H; OCH_3), 3.12 (s, 2H; CH_2), 1.29 (t, ^3J(H,H) = 7 Hz, 3H; CH_3CH_2); ^{13}C NMR (200 MHz, $CDCl_3$): δ = 170.7 (CO), 156.0 (C=CH_2), 84.5 (CH_2=C), 63.2 (CH_2O), 52 (CH_3O), 41 (CH_2), 14.3 (CH_2CH_3). GC-MS: *m/z* = 144 (13), 113 (6), 101 (5), 85 (17), 84 (17), 74 (42), 59 (23), 56 (36), 43 (100), 42 (51), 41 (9), 40 (7), 39 (21).

Methyl (*E*)-3-ethoxy-2-butenoate ((*E*)-7): ^1H NMR (200 MHz, $CDCl_3$): δ = 5.00 (s, 1H; CH), 3.82 (q, ^3J(H,H) = 7 Hz, 2H; OCH_2), 3.67 (s, 3H; OCH_3), 2.30 (s, 3H; CH_3), 1.34 (t, ^3J(H,H) = 7 Hz, 3H; CH_3CH_2); ^{13}C NMR (200 MHz, $CDCl_3$): δ = 172.6 (C=CH), 168.5 (C=O), 90.6 (CH), 63.7 (CH_2O), 50.7 (CH_3O), 19.1 (CH_3), 14.2 (CH_2CH_3). GC-MS: *m/z* = 144 (9), 113 (27), 101 (38), 85 (73), 84 (28), 69 (57), 59 (17), 43 (100), 42 (15), 41 (13), 40 (9), 39 (26). The (^1H and ^{13}C) NMR data are in good agreement with the literature values for analogous compounds [18].

Methyl (*Z*)-3-ethoxy-2-butenoate ((*Z*)-7): ^1H NMR (200 MHz, $CDCl_3$): δ = 4.90 (q, ^4J(H,H) = 0.7 Hz, 1H; CH), 4.11 (q, ^3J(H,H) = 7 Hz, 2H; OCH_2), 3.65 (s, 3H; OCH_3), 2.01 (d, ^4J(H,H) = 0.7 Hz, 3H; CH_3), 1.37 (t, ^3J = 7 Hz, 3H; CH_3CH_2); ^{13}C NMR (200 MHz, $CDCl_3$): δ = 167.7 (C=CH), 165.9 (C=O), 95.5 (CH), 64.7 (CH_2O), 50.5 (CH_3O), 19.6 (C4) 15.2 (CH_3CH_2). GC-MS was identical with that of (*E*)-**7**.

2,2-Dimethyl-5-(1-ethoxyethylidene)-1,3-dioxane-4,6-dione (11): **11** was synthesized by analogy with the method of Bihlmayer [42]. Meldrum's acid (2.5 g, 2.42×10^{-2} mol) was dissolved in an excess of triethyl orthoacetate (16 mL, 8.2×10^{-2} mol) under N_2. The solution was stirred and heated at 80 °C for 3 h. The yellow solution was then cooled overnight. The solid was filtered and recrystallized from CCl_4 to give **8** as white crystals (1.73 g, 8.08×10^{-3} mol); m.p. 86–88 °C, yield 33%. ^1H NMR (200 MHz, $CDCl_3$): δ = 4.40 (q, ^3J(H,H) = 7 Hz, 2H; CH_2), 2.73 (s, 3H; CH_3), 1.70 (s, 6H; $2 \times (CH_3)$), 1.51 (t, ^3J(H,H) = 7 Hz, 3H; CH_2-CH_3); ^{13}C NMR (200 MHz, $CDCl_3$): δ = 186.2 (C7), 163.5 (C=O), 159.4 (C=O), 102.6 (C2), 97.5 (C5), 67 (OCH_2), 26.9 ($2 \times (CH_3)$), 18.3 (CH_3), 14.7 (CH_3CH_2). Anal. calcd. for $C_{10}H_{14}O_5$: C, 56.07; H, 6.54. Found: C, 56.02; H, 6.65.

Trapping of 12 with methanol: 11 (270 mg) was sublimed at 62 °C (3×10^{-5} mbar) and thermolyzed through the 40 cm oven at 475 °C onto a cold finger coated with methanol and cooled to −196 °C. After the end of the reaction, (*E*)-**7** was isolated by column chromatography (SiO_2, $CHCl_3$); yield 62%. HRMS calcd. for $C_7H_{13}O_3$: *m/z* 144.0786, found 144.0782.

Ethyl allenecarboxylate (5b): The synthesis of **5b** was described by Hamlet and Barker [40]. **5b** was vaporized at −40 °C (10^{-5} mbar). IR (neat, −196 °C): $\tilde{\nu}$ = 3036 (vw), 2984 (w), 1971 (m), 1941 (w), 1711 (s), 1424 (w), 1369 (m), 1337 (m), 1302 (w), 1277 (m), 1266 (m), 1260 (m), 1184 (m), 1095 (w), 1036 (w), 953 (w), 860 (m), 781 (m) cm^{-1}; IR (Ar matrix, 12 K): $\tilde{\nu}$ = 3004 (w), 2987 (w), 1985 (m), 1979 (m), 1943 (m), 1745 (m), 1737 (s), 1732 (s), 1726 (s), 1714 (s), 1483 (w), 1449 (w), 1430 (w), 1371 (m), 1345 (m), 1299 (m), 1286 (s), 1272 (m), 1270 (s), 1268 (s), 1257 (s), 1194 (s), 1178 (s),

0947-6539/97/0302-0246 $ 15.00+.25/0 Chem. Eur. J. 1997, 3, No. 2

1175 (s), 1162 (m), 1101 (w), 1045 (m), 1038 (m), 1035 (m), 950 (w), 884 (w), 868 (m), 843 (s), 777 (w) cm^{-1}.

***N,N*-3-Dimethylaminocyclobutenone (3c)**: In a two-neck flask, 1,3-cyclobutanedione [13] (0.42 mg, 5.10^{-3} mol) was added to a dry solution of CH_2Cl_2 (25 mL) under N_2. The solution was then cooled to 0 °C. A fresh solution of dimethylamine (1 equiv.) in dry THF was added dropwise. The solution was stirred at 0 °C for 2 h. After removing solvents, **3c** was purified by column chromatography (1:9 MeOH:$CHCl_3$) to give (0.410 mg, 3.7×10^{-3} mol); yield 74%. **3c** was vaporized at 60 °C (10^{-5} mbar). ^{1}H NMR (200 MHz, $CDCl_3$): $\delta = 4.61$ (s, 1H; CH), 3.14 (s, 2H; CH_2), 3.10 (s, 3H; CH_3), 3.04 (s, 3H; CH_3); ^{13}C NMR (200 MHz, $CDCl_3$): $\delta = 180.0$ (C=O), 169.4 (C3), 98.9 (CH), 45.9 (CH_2), 40 (CH_3), 38.8 (CH_3); IR (neat, −196°C): $\tilde{\nu}$ = 2976 (w), 1726 (w), 1706 (w), 1601 (s), 1454 (w), 1429 (m), 1381 (w), 1324 (vw), 1292 (w), 1158 (w), 1079 (w), 1050 (w), 1006 (w), 912 (w), 879 (w), 762 (w), 753 (w) cm^{-1}; IR (Ar, 14 K): $\tilde{\nu}$ = 3011 (w), 2955 (w), 2934 (w), 2911 (w), 1772 (m), 1722 (w), 1622 (s), 1611 (m), 1593 (m), 1590 (m), 1476 (w), 1453 (w), 1433 (w), 1419 (w), 1391 (w), 1362 (w), 1217 (w), 1164 (w), 1148 (w), 1065 (w), 1038 (w), 994 (w), 910 (w), 767 (w), 764 (w) cm^{-1}. MS: m/z = 111 (100), 68 (26), 67 (11), 55 (19), 43 (21), 42 (22), 39 (9). HRMS: calcd. for C_6H_9NO: m/z 111.0684, found 111.0683.

***N,N*-Dimethylamino allenecarboxamide (5c)**: A solution of dimethylamine in THF (0.6 mL; 3.92×10^{-3} mol; 6.48 M) was added to 25 mL of dry THF under N_2. The solution was then cooled to −50 °C. 2,3-Butadienoyl chloride [25a] (**5d**) (0.2 g; 1.96 10 − 3 mol) was added dropwise to the cold, stirred solution. After 1 h of stirring at −50 °C, the solution was warmed to −25 °C and kept at this temperature for 3 h. Without stirring, the solution was then warmed to 0 °C. The pH was checked. If the solution was slightly acidic, potassium carbonate was added until neutralization. After filtration and evaporation of solvents, ether was added, and once more filtration was carried out to remove completely the ammonium salt formed. After evaporation of the solvent, a mixture of 2:1 petroleum ether (b.p. 30–40 °C):ether was added to the viscous oil. After a night in a freezer, **5c** (0.11 g, 9.8 10^{-4} mol) crystallizsed as white needles, mp 41–42 °C; yield 50%. **5c** was sublimed at 0 °C (10^{-5} mbar). ^{1}H NMR (200 MHz, $CDCl_3$): $\delta = 5.95$ (t, ^4J(H,H) = 6.6 Hz, 1H; CH), 5.15 (d, ^4J(H,H) = 6.6 Hz, 2H; CH_2), 3.09 (s, 3H; NCH_3), 3.00 (s, 3H; NCH_3); ^{13}C NMR ($CDCl_3$): 213.4 (C3), 164.8 (C=O), 87.3 (CH), 78.7 (CH_2=C), 38 (NCH_3), 35.8 (NCH_3); IR (neat, −196 °C): $\tilde{\nu}$ = 3049 (w), 2969 (w), 1969 (w), 1948 (m), 1617 (s), 1500 (m), 1398 (m), 1260 (w), 1153 (m), 1092 (w), 1062 (w), 857 (m), 763 (w) cm^{-1}; IR (Ar, 12 K): $\tilde{\nu}$ = 2953 (w), 2936 (w), 2919 (w), 2898 (w). 2880 (w), 2863 (w), 2855 (w), 1978 (m), 1949 (w), 1663 (s), 1655 (m), 1653 (m), 1501 (m), 1465 (w), 1453 (w), 1437 (w), 1424 (w), 1401 (m), 1393 (m), 1368 (w), 1362 (w), 1354 (w), 1265 (w), 1217 (w), 1194 (w), 1180 (w), 1130 (m), 1086 (w), 1070(w), 1062 (w), 983 (w), 973 (w), 859 (w), 844 (m), 842 (m), 840 (m), 759 (w) cm^{-1}. GC-MS: m/z = 111 (13), 83 (7), 82 (7), 72 (100), 68 (17), 67 (19), 55 (30), 44 (43), 42 (57), 39 (70); Anal. calcd. for C_6H_9NO: C, 64.86; H, 8.11; N, 12.61. Found: C, 64.57; H, 8.36; N, 12.59.

2,3-Butadienoyl Chloride (5d): The procedure was as described by Brown et al. [25a]. **5d** was vaporized at −40 °C (10^{-5} mbar). ^{1}H NMR (200 MHz, $CDCl_3$): $\delta = 5.93$ (t, ^4J(H,H) = 6.2 Hz, 1H; CH), 5.49 (d, ^4J(H,H) = 6.2 Hz, 2H, CH_2); ^{13}C NMR ($CDCl_3$): $\delta = 219.3$ (C3), 164.7 (C=O), 95.5 (CH), 81.6 (CH_2); IR (neat, −196 °C): $\tilde{\nu}$ = 3072 (w), 2994 (w), 1962 (m), 1914 (w), 1848 (w), 1795 (w), 1755 (s), 1748 (s), 1720 (m), 1135 (m), 1040 (m), 978 (w), 923 (w), 910 (w), 856 (m), 787 (w) cm^{-1}; IR (Ar, 12 K): $\tilde{\nu}$ = 3013 (w), 1969 (m), 1925 (w), 1850 (w), 1847 (w), 1841 (w), 1836 (w), 1786 (w), 1775 (w), 1773 (m), 1770 (s), 1760 (w), 1502 (vw), 1411 (w), 1328 (w), 1318 (w), 1137 (w), 1126 (m), 1093 (vw), 1086 (vw), 1039 (m), 1002 (w), 970 (m), 859 (w), 856 (m), 851 (m), 849 (m), 799 (w), 785 (w) cm^{-1}.

Methyl 3-Chloro-3-butenoate [26] (**17**): **5d** (200 mg) was vaporized at −40 °C (2×10^{-5} mbar) and thermolyzed through the 40 cm oven at 550 °C onto a cold finger coated with methanol and cooled to −196 °C. After the end of the reaction, **17** was isolated in 74% yield. Data are in good agreement with the literature values [26]. ^{1}H NMR (200 MHz, $CDCl_3$): $\delta = 5.39$ (d, ^2J(H,H) = 1.6 Hz, 1H; (*E*)-H4), 5.36 (m, 1H; (*Z*)-H4), 3.75 (s, 3H; CH_3), 3.38 (d, ^3J(H,H) = 0.9 Hz; CH_2); ^{13}C NMR (200 MHz, $CDCl_3$): $\delta = 169.1$ (C=O), 134.1 (C-Cl), 116.6 (CH_2vyn), 52.2 (CH_3), 44.3 (CH_2). GC-MS: m/z = 136 (9), 134 (19), 106 (42), 103 (85), 99 (41), 75 (19), 69 (11), 67 (11), 59 (23), 43 (43), 39 (100).

Acknowledgments: We thank the Australian Research Council for financial support (to C. W.) and for a research fellowship for M. W. W., The University of Queensland for generous allocations of computer time, and G. Macfarlane for the FVP-MS experiments. C. W. thanks the Institute for Fundamental Research in Organic Chemistry, Kyushu University, Japan, for its hospitality during the editing of this manuscript.

Received: July 23, 1996 [F419]

[1] a) T. T. Tidwell, *Ketenes*; Wiley: New York, **1995**; b) C. Wentrup, W. Heilmayer, G. Kollenz, *Synthesis* **1994**, 1219–1248; c) J. Hyatt, P. W. Raynolds, *Org. Reactions* **1994**, *45*, 159; d) E. Schaumann, S. Scheiblich in *Houben-Weyl, Methoden der Organischen Chemie*, Thieme Verlag, Stuttgart, **1993**, Vol. E15/2, pp. 2353–2530 and 2818–2881; e) T. T. Tidwell, *Acc. Chem. Res.* **1990**, *23*, 273–279; f) *The Chemistry of Ketenes, Allenes and Related Compounds* (S. Patai), Wiley, New York, **1980**.

[2] a) C. Wentrup, K.-P. Netsch, *Angew. Chem. Int. Ed. Engl.* **1984**, *23*, 802; b) C. Wentrup, H.-W. Winter, G. Gross, K.-P Netsch, G. Kollenz, W. Ott, G. Biedermann, *ibid.* **1984**, *23*, 800–802.

[3] a) M. W. Wong, C. Wentrup, *J. Org. Chem.* **1994**, *59*, 5279–5285; b) Cf. also D. M. Birney, *J. Org. Chem.* **1996**, *61*, 243–251; R. Koch, M. W. Wong, C. Wentrup, *ibid.* **1996**, *61*, 6809–6813.

[4] a) A. Ben Cheikh, J. Chuche, N. Manisse, J. C. Pommelet, K.-P Netsch, P. Lorencak, C. Wentrup, *J. Org. Chem.* **1991**, *56*, 970–975; b) C. O. Kappe, G. Kollenz, R. Leung-Toung, C. Wentrup, *J. Chem. Soc. Chem. Commun.* **1992**, 487–488; c) B. Fulloon, H. A. A. El-Nabi, G. Kollenz, C. Wentrup, *Tetrahedron Lett.* **1995**, *36*, 6547–6550; d) B. Fulloon, C. Wentrup, *J. Org. Chem.* **1996**, *61*, 1363–1368. e) C. Wentrup, B. E. Fulloon, D. W. J. Moloney, H. Bibas, M. W. Wong, *Pure Appl. Chem.* **1996**, *68*, 891–894.

[5] a) M. W. Wong, C. Wentrup, unpublished results; b) S. Ham, D. M. Birney, *J. Org. Chem.* **1996**, *61*, 3962–3968.

[6] Preliminary communication: H. Bibas, M. W. Wong, C. Wentrup, *J. Am. Chem. Soc.* **1995**, *117*, 9582–9583.

[7] G. B. Stone, L. S. Liebeskind, *J. Org. Chem.* **1990**, *55*, 4614–4622.

[8] a) C. O. Kappe, M. W. Wong, C. Wentrup, *J. Org. Chem.* **1995**, *60*, 1686–1695; b) R. H. Zuhse, M. W. Wong, C. Wentrup, *J. Phys. Chem.* **1996**, *100*, 3917–3922.

[9] All molecules having the structures **1** or **2** are defined as *s-trans*, regardless of the nature of R.

[10] a) The corrected ratio (*s-cis*/*s-trans*) between the *s-cis* and *s-trans* forms was derived by multiplying the observed intensity ratio of well-resolved peaks of the two conformers in the 1200–1300 cm^{-1} region by the calculated ratio of their extinction coefficients ($\varepsilon_{s-trans}/\varepsilon_{s-cis}$) obtained at the B3-LYP/6-31G* level. It ignores the unknown errors in the calculated ε values; b) The calculated energy barrier separating *s-trans*-**4a** and *s-cis*-**4a** is 19 kJ mol^{-1}, which means that they will not interconvert in the low temperature matrix. The calculated energy difference (at 10 K) is +8 kJ mol^{-1} (G2(MP2,SVP); cf. Section 4). This would give a ratio of *s-trans*-**4a**:*s-cis*-**4a** of the order of 10^6 and a conversion rate of the order of 10^4 s^{-1} at 70 K.

[11] G. C. Pimentel, S. W. Charles, *Pure Appl. Chem.* **1963**, *7*, 111.

[12] a) G. C. Pimentel, C. B. Moore, *J. Chem. Phys.* **1963**, *38*, 2816–2829; b) J. Wirz, R. Hochstrasser, *Angew. Chem. Int. Ed. Engl.* **1990**, *29*, 411–413.

[13] H. H. Wasserman, J. U. Piper, E. V. G. Dehmlow, *J. Org. Chem.* **1973**, *38*, 1451–1455.

[14] T. L. Jacobs, R. Cramer, J. H. Hanson, *J. Am. Chem. Soc.* **1942**, *64*, 223–226.

[15] All the bands observed were in very good agreement with the literature [12].

[16] J. K. Terlouw, P. C. Burgers, J. L. Holmes, *J. Am. Chem. Soc.* **1979**, *101*, 225–226.

[17] a) X. Duan, M. Page, *J. Am. Chem. Soc.* **1995**, *117*, 5114–5119; b) Y. Chiang, H.-X. Guo, A. J. Kresge, O. S. Tee, *ibid.* **1996**, *118*, 3386–3391; c) J. Frey, Z. Rappoport, *ibid.* **1996**, *118*, 5182–5191; d) D. J. Graham, S. M. Hurst, J.-C. Luo, *J. Phys. Chem.* **1995**, 99, 1115–1119; e) M. T. Nguyen, D. Sengupta, G. Raspoet, L. G. Vanquickenborne, *ibid.* **1995**, 99, 11883–11888.

[18] E. Taskinen, V-M. Mukkala, *Tetrahedron* **1982**, *38*, 613–616.

[19] Cf. A. Ben Cheik, H. Dhimane, J. C. Pommelet, J. Chuche, *Tetrahedron Lett.* **1988**, *29*, 5919.

[20] *s-cis*-Acetylketene: $\tilde{\nu}$ = 3095, 2148, 2143, 1681, 1378, 1345, and 1168 cm^{-1}. *s-trans*-Acetylketene: $\tilde{\nu}$ = 3083, 2137, 2133, 1699, 1343, and 1221 cm^{-1}.

[21] a) An extra peak at 2130 cm^{-1} is also observed due to the formation of unsubstituted vinylketene in a retroene reaction, which will be described in a separate paper [21b]. b) H. Bibas, R. Koch, C. Wentrup, unpublished results.

[22] a) cf. R. Leung-Toung, C. Wentrup, *Tetrahedron* **1992**, *48*, 7641–7654; b) Propyne formation from **5b** may involve elimination of ethene to give allene carboxylic acid, followed by known decarboxylation to give propyne: J. W. Dallinga, N. M. M. Nibbering, A. J. H. Boerboom, J. *Chem. Soc. Perkin Trans 2*, **1983**, 281–284; c) The formation of propyne could also be expained by decarboxylation to allene itself, followed by isomerization to propyne, but only a minute band due to unsubstituted allene (1955 cm^{-1}) was formed from **5b** at 900 °C.

[23] a) FVT-MS was carried out on **5b**. From 570 to 650 °C the peaks at $m/z = 84$ and 28 increased in intensity due to the formation of **8** and ethene. Above 650 °C, **8** started to decrease, in contrast to $m/z = 28$ (ethene), which continued to increase. At the same time, peaks at $m/z = 44$ and 40 due to CO_2 and propyne, respectively, increased drastically. b) The FVT-MS technique (Kratos MS 25 RFA) is described in C. Wentrup, P. Kambouris, R. A. Evans, D. Owen, G. Macfarlane, J. Chuche, J. C. Pommelet, A. Ben Cheikh, M. Plisnier, R. Flammang, *J. Am. Chem. Soc.* **1991**, *113*, 3130–3135.

[24] The experimental IR spectrum agrees well with B3-LYP/6-31G* calculations for a mixture of *s-cis*- and *s-trans*-**4c** (obsvd: 2957 (vw), 2863 (vw), 2846 (vw), 2132 (vs), 1635 (s), 1457 (w), 1458 (w), 1320 (w), 1362 (w), 1217 (m), 1156 (m), 1145 (m), 1060 (w), 1013 (m), 807 (w), 767 (m) cm^{-1}).

[25] a) R. F. C. Brown, K. J. Coulston, F. W. Eastwood, A. D. E. Pullin, A. C. Staffa, *Aust. J. Chem.* **1990**, *43*, 561–577; b) Cf. G. Himbert, H.-J. Schlindwein, *Z. Naturforsch.* **1992**, *47b*, 1785–1793.

[26] T. Nogi, J. Tsuji, *Tetrahedron* **1969**, *25*, 4099–4108.

[27] H. Brouwer, J. B. Stothers, *Can. J. Chem.* **1972**, *50*, 601–611.

[28] a) 3-Chlorocyclobutenone is calculated to lie 13 kJ mol^{-1} *above* ketene *s-trans*-**4d** and 4 kJ mol^{-1} above *s-cis*-**4d** (G2(MP2,SVP)); b) In the methoxy case, **3a** is calculated to be 4 kJ mol^{-1} below *s-trans*-**4a**, and 8 kJ mol^{-1} below *s-cis*-**4a**; c) In the dimethylamino case, **3c** is calculated to be 29 kJ mol^{-1} below *s-trans*-**4c** and 32 kJ/mol below *s-cis*-**4c**.

[29] a) B. J. Smith, L. Radom, *J. Phys. Chem.* **1995**, *99*, 6468–6471; b) L. A. Curtiss, P. C. Redfern, B. J. Smith, L. Radom, *J. Chem. Phys.* **1996**, *104*, 5148–5152.

[30] M. W. Wong, *Chem. Phys. Lett.* **1996**, *256*, 391–399.

[31] a) J. Goerdeler, K. Jonas, *Chem. Ber.* **1966**, *99*, 3572–3577; b) J. Goerdeler, D. Wobig, *Liebigs Ann. Chem.* **1970**, *731*, 120–141; c) J. Goerdeler, H.-J. Bartsch, *Chem. Ber.* **1985**, *118*, 2294–2299, 4196–4202.

[32] a) G. Himbert, D. Fink, *Z. Naturforsch.* **1994**, *49b*, 542–550; b) G. Himbert, D. Fink, *J. Prakt. Chem.* **1994**, *336*, 654–657.

[33] W. J. Hehre, L. Radom, P. v. R. Schleyer, J. A. Pople, *Ab Initio Molecular Orbital Theory*; Wiley, New York, **1986**.

[34] a) *Density Functional Methods in Chemistry* (Eds.: J. K. Labanowski, J. W. Andzelm), Springer, New York, **1991**; b) *Modern Density Functional Theory; A Tool for Chemistry* (Eds.: J. M. Seminario, P. Politzer), Elsevier, Amsterdam, **1995**.

[35] M. J. Frisch, G. W. Trucks, H. B. Schlegel, P. M. W. Gill, B. G. Johnson, M. W. Wong, J. B. Foresman, M. A. Robb, M. Head-Gordon, E. S. Replogle, R. Gomperts, J. L. Andres, K. Raghavachari, J. S. Binkley, C. Gonzalez, R. L. Martin, D. J. Fox, D. J. DeFrees, J. Baker, J. J. P. Stewart, J. A. Pople, Gaussian 92/DFT, Gaussian, Pittsburgh PA, **1993**.

[36] a) A. D. Becke, *J. Chem. Phys.* **1993**, *98*, 5648–5652; b) C. Lee, W. Yang, R. G. Parr, *Phys. Rev. B* **1988**, *37*, 785–789.

[37] C. Wentrup, R. Blanch, H. Briehl, G. Gross, *J. Am. Chem. Soc.* **1988**, *110*, 1874–1880.

[38] C. D. Hurd, *Syn. Coll. Vol. 1*, **1941**, 330–334.

[39] C. D. Hurd, J. W. Williams, *J. Org. Chem.* **1940**, *5*, 122–125.

[40] Z. Hamlet, W. D. Barker, *Synthesis* **1970**, 543–544.

[41] R. W. Lang, H.-J. Hansen, *Helv. Chim. Acta* **1980**, *63*, 438–455.

[42] G. A. Bihlmayer, G. Derflinger, J. Derkosch, O. E. Polansky, *Monatsh. Chem.* **1967**, *98*, 564.

 0947-6539/97/0302-0248 $ 15.00+.25/0